Synthesis and Dielectric Properties of Polyimide-Tethered Polyhedral Oligomeric Silsesquioxane (POSS) Nanocomposites via POSS-diamine

Chyi-Ming Leu, Yao-Te Chang, and Kung-Hwa Wei*

Department of Materials Science and Engineering, National Chiao Tung University, Hsinchu, Taiwan 30049, R.O.C.

Received June 2, 2003; Revised Manuscript Received September 18, 2003

ABSTRACT: Polyimide-tethered polyhedral oligomeric silsesquioxane, ($R_7R'Si_8O_{12}$) (POSS), nanocomposites with well-defined architectures are prepared by the copolymerization reaction of a new type of diamine monomer: POSS-diamine, 4,4′-oxydianiline (ODA), and pyromellitic dianhydride (PMDA). This type of polyimide-side-chain-tethered POSS nanocomposite presents self-assembly characteristics when the amount of POSS exceeds10 mol %, as evidenced by transmission electron microscopy studies. Furthermore, POSS/polyimide nanocomposites have both lower and tunable dielectric constants, with the lowest value of 2.3, and controllable mechanical properties, as compared to that of pure polyimide.

Introduction

Polyimides are synthesized by the polycondensation reaction of dianhydride and diamine monomers and are well-known for their strength and high-temperature durability (service temperatures can exceed 400 °C). They can be used as interlayer dielectrics in microelectronics applications by simple spin-coating techniques.[1] The dielectric constants of most polyimides are between 3.1 and 3.5; further reduction in the dielectric constant of these materials is needed to avoid cross-talk between conducting wires as electronic devices continue to shrink. A variety of approaches to physically and chemically alter the structure of polyimides to obtain lower dielectric constants have been attempted. The synthesis of fluorinated polyimides has been one such approach.[2−4] Although the dielectric constant of fluorinated polyimide is lower (about 2.6), poor mechanical properties and high monomer costs compromise its use. A second approach has been to introduce voids in polyimides by thermal degradation of the poly(propylene oxide) block of a phase-separated polyimide−poly(propylene oxide) block copolymer.[5,6] A substantial reduction in the dielectric constant of polyimide can be obtained (2.3−2.5). In this approach, however, it is critically important to completely remove the residual organic compound and produce uniform, controllable, and closed pores.

We wonder whether, in another approach, preformed and uniform nanoporous inorganic species can be incorporated into polyimide to reduce the dielectric constant without detrimentally affecting the mechanical properties of polyimide. Polyhedral oligomeric silsesquioxanes have been demonstrated to be building blocks for the formation of organic−inorganic nanocomposite materials for various applications, owing to the ease with which functional groups can be attached on polyhedral oligomeric silsesquioxanes.[7−22] For instance, polyhedral oligomeric silsesquioxanes can be used as monofunctional or graftable monomers, difunctional comonomers, surface modifiers, or polyfunctional crosslinkers for the formation of polymers. We suggest that one member of the polyhedral oligomeric silsesquioxane family, octamer $(RSiO_{1.5})_8$, which consists of a rigid and cubic silica core with a nanopore diameter of about 0.3−0.4 nm,[7] is a possible candidate. The incorporation of $(RSiO_{1.5})_8$ into some polymers has led to enhancements in their thermal stability and mechanical properties,[8,9,12] such as in the case of acrylics,[8] styryls,[10] epoxies,[11,15,18] and polyethylene.[21] One variation of $(RSiO_{1.5})_8$ is ($R_7R'Si_8O_{12}$), where R and R′ represent nonreactive and reactive groups, respectively; this structure is termed POSS in the present study.

Previously, we have demonstrated that covalently tethering nanoporous POSS to presynthesized polyimide chain ends[23] or the side chains[24] results in organic−inorganic nanocomposite materials with much lower dielectric constants and controllable mechanical properties. The approach has limitations because it requires particular functional groups to be present in polyimide to react with POSS.

Here, we adopt a copolymer approach to directly synthesize polyimide-tethered POSS by the copolymerization of a newly developed diamine monomer, POSS-diamine, along with other diamines and dianhydride monomers. This copolymer approach provides a versatile way to design a variety of polyimide nanocomposites with a wide range of dielectric constants and mechanical properties. Furthermore, the molar ratio of POSS-diamine is adjustable, and this in turn produces nanocomposites with tunable dielectric constants. Polyimide molecules offer the advantage of both high thermal and mechanical strengths.

The synthesis of the diamine monomer containing the POSS structure is presented in Scheme 1. First, cyclopentyltrisilanol-POSS was reacted with trichloro[4-(chloromethyl)phenyl]silane to form a POSS with a benzyl chloride functional group (POSS-Cl). Nucleophilic substitution of the chloride functional group of POSS-Cl with 4-hydroxybenzaldehyde was carried out in a K_2CO_3/DMF/THF medium to give POSS-aldehyde. POSS-aldehyde was then reacted with aniline to form a POSS compound with two amino functional groups, which is termed POSS-diamine in this study.

Various proportions of POSS-diamine monomer and 4,4′-oxydianiline (ODA)were reacted with pyromellitic dianhydride (PMDA) to form copoly(amic acid) in NMP/

* To whom correspondence should be addressed: Tel 886-35-731871, Fax 886-35-724727, e-mail khwei@cc.nctu.edu.tw.

10.1021/ma034743r CCC: $25.00
Published on Web 10/28/2003

Scheme 1

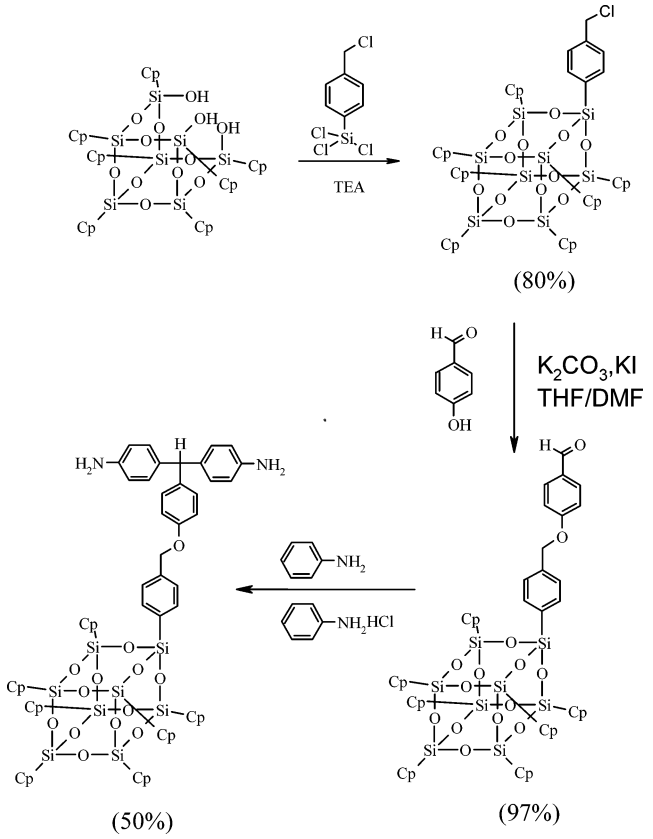

Scheme 2

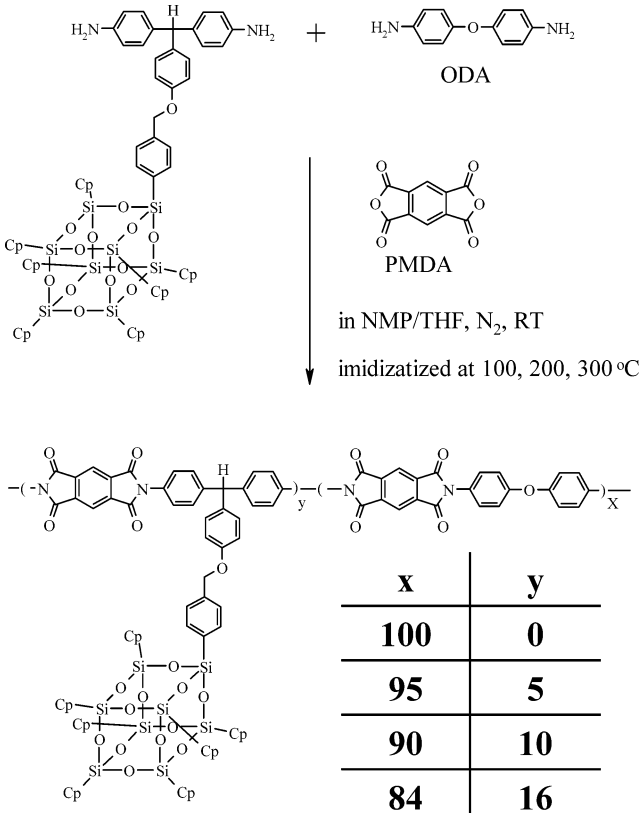

x	y
100	0
95	5
90	10
84	16

THF cosolvent with different amounts of POSS, as shown in Scheme 2.

Experiment

Materials. Cyclopentyltrisilanol-POSS was obtained from Hybrid Plastics Co., and all solvents used were obtained from Aldrich. Pyromellitic dianhydride (PMDA) and 4,4′-oxydianiline (ODA) were purchased from TCI in Tokyo, Japan.

POSS-Cl. POSS-Cl was prepared by reacting trichloro[4-(chloromethyl)phenyl]silane (1.0 mL, 5.61 mmol) with cyclopentyltrisilanol-POSS (5.00 g, 5.11 mmol) in the presence of triethylamine (2.2 mL, 15.41 mmol) in 30.0 mL of dry THF. The reaction flask was stirred under nitrogen for 2 h, followed by filtration to remove the $HNEt_3Cl$ byproduct. The clear THF solution was dropped into a beaker of acetonitrile and rapidly stirred. The resulting product was collected by filtration and dried in a vacuum. (4.61 g, 80%).

^{1}H NMR ($CDCl_3$): δ7.59 (d, J = 7.5 Hz, 2H), 7.33 (d, J = 7.5 Hz, 2H), 4.52 (s, 2H), 1.75−1.72 (m, 14H), 1.57−1.48 (m, 42H), 1.04−0.96 (m, 7H).

POSS-aldehyde. 4-Hydroxybenzaldehyde (0.14 g, 1.06 mmol) and K_2CO_3 (0.32 g, 0.98 mmol) were mixed in DMF (10.0 mL), and the reaction mixture was heated at 80 °C under a nitrogen atmosphere for 1 h. POSS-Cl (1.00 g, 0.80 mmol) was dissolved in dry THF (10.0 mL) and added dropwise over a period of 0.5 h to the mixture. NaI (0.14 g, 0.98 mmol) was added to the reaction mixture, and heating was continued for 4 h. The solution was diluted with water and extracted with dichloromethane (3 × 15.0 mL). The extracted organic layer was washed with water two times (2 × 50.0 mL) and concentrated in a vacuum to furnish POSS-aldehyde as a light white powder (1.01 g, 97%).

^{1}H NMR ($CDCl_3$, δ ppm): 9.87 (s, J = 9.0 Hz, 1H), 7.82 (d, J = 8.7 Hz, 2H), 7.69 (d, J = 8.1 Hz, 2H), 7.41 (d, J = 8.1 Hz, 2H), 7.06 (d, J = 8.1 Hz, 2H), 5.16 (s, 2H), 1.75−1.72 (m, 14H), 1.57−1.48 (m, 42H), 1.04−0.96 (m, 7H). ^{13}C NMR ($CDCl_3$, δ ppm): 190.9, 163.9, 138.1, 134.7, 132.6, 132.2, 130.5, 126.7, 115.4, 70.4, 27.5, 27.2, 27.1, 22,5, 22.4. ^{29}Si NMR (THF, δ ppm): −67.9, −68.2, −79.6. MS (m/z): found, 1112.0; calculated, 1110.3 for $C_{49}H_{74}O_{14}Si_8$.

POSS-diamine. POSS-aldehyde (1.22 g, 10.0 mmol), aniline (3.14 g, 34.5 mmol), and aniline hydrochloride (0.08 g, 0.59 mmol) were dissolved at 110 °C under a nitrogen atmosphere. The mixture was heated at 150 °C for 1.5 h. The reaction mixture was then cooled to room temperature, and the excess aniline was distilled in a vacuum. The residue was dissolved in 1 M aqueous hydrochloric acid solution and treated with 10 wt % aqueous sodium hydroxide solution until the precipitate dissolved. This solution was then washed with 100 mL of ether three times. Subsequently, the aqueous phase was neutralized with 1 M hydrochloric acid aqueous solution, and the precipitate was collected by filtration and dried. The product was purified by flash column chromatography (methylene chloride/ethyl acetate/methanol 80:18:2) to give purple red needles (50%).

^{1}H NMR ($CDCl_3$, δ ppm): 7.66 (d, J = 8.4 Hz, 2H), 7.40 (d, J = 8.4 Hz, 2H), 6.99 (d, J = 8.4 Hz, 2H), 6.87 (d, J = 8.4 Hz, 2H), 6.85 (d, J = 8.4 Hz, 4H), 6.60 (d, J = 8.4 Hz, 4H), 5.28 (s, 2H), 5.01 (s, 2H), 1.85−1.75 (m, 14H), 1.57−1.48 (m, 42H), 1.04−0.98 (m, 7H). ^{13}C NMR ($CDCl_3$, δ ppm): 157.0, 144.2, 139.2, 137.6, 135.1, 134.3, 131.7, 130.2, 130.1, 126.5, 115.0, 114.4, 69.9, 27.3, 27.0, 26.9, 22,2, 22.1. ^{29}Si NMR (THF, δ ppm): −67.9, −68.2, −79.6. MS (m/z): found, 1279.1; calculated, 1278.4 for $C_{61}H_{86}O_{13}Si_8N_2$.

Preparation of PMDA-ODA and POSS/PMDA-ODA. Poly(amic acid) (PAA) of PMDA-ODA was synthesized by first putting 10.00 mmol of ODA into a three-necked flask containing 22.92 g of NMP/10.00 g of THF under nitrogen purge at 25 °C. Then, after ODA had dissolved completely, 10.20 mmol of PMDA, divided into three batches, was added to the flask batch-by-batch with a time interval of 0.5 h between batches. When PMDA had completely dissolved in the solution, the solution was stirred continuously for 1 h, and a viscous PAA solution was obtained. The mixture was then mixed for an additional 12 h using a mechanical stirrer. The final content of PAA in NMP/THF was 11 wt %.

PMDA-(ODA/POSS-diamine) copoly(amic acid) was synthesized using the same method for PMDA-ODA, except that

Table 1. Elemental Analysis of POSS/Polyimide Nanocomposites

mol % of POSS in polyimide	intrinsic viscosities (dL/g)	elemental analysis			wt % of POSS in polyimide[a] (%)	vol % of POSS[b] (%)
		C %	H %	N %		
0	1.4	67.5	3.1	7.5	0	0
5	1.1	65.0	3.5	6.7	14.2	18.2
10	1.2	63.0	3.9	6.1	26.6	32.8
16	1.3	56.5	4.2	4.8	39.4	46.6

[a] The weight percentage (wt %) of POSS in polyimide was calculated from the elemental analysis results of pure polyimide and POSS/polyimide nanocomposites. [b] The densities of POSS and polyimide are approximately 1.12 and 1.48 g/cm^3, respectively.

various proportions of POSS-diamine were added. The final content of copoly(amic acid) in NMP/THF was also 11 wt %. For instance, the copoly(amic acid) of 5 mol % POSS/PMDA-ODA was prepared by first putting 0.5 mmol (0.64 g) of POSS-diamine and 9.50 mmol (1.9 g) of ODA into a three-necked flask containing 28.60 g of NMP/10.00 g of THF under nitrogen purge at 25 °C. Then, after POSS-diamine and ODA had dissolved completely, 10.20 mmol (2.22 g) of PMDA, divided into three batches, was added to the flask batch-by-batch with a time interval of 0.5 h between batches. When PMDA had completely dissolved in the solution, the solution was stirred continuously for 1 h and a viscous PAA solution was obtained. The mixture was then mixed for an additional 12 h using a mechanical stirrer.

The PAA of PMDA-ODA and PMDA-ODA/POSS-diamine mixture were cast on glass slides using a doctor blade and subsequently put in a vacuum oven at 40 °C for 48 h before the imidization step. Imidization of PMDA-ODA and POSS-PMDA-ODA was carried out by putting the samples in an air-circulation oven at 100, 150, 200, and 250 °C for 1 h and then at 300 °C for 0.5 h to ensure complete imidization.

Characterization. ^{1}H and ^{13}C NMR spectra were recorded on a Varian Unity-300 NMR spectrometer. ^{29}Si NMR spectra were obtained from a DMX-600 NMR spectrometer. Matrix-assisted laser desorption/ionization (MALDI) mass spectra were recorded on a linear time-of-flight mass spectrometer (TOF MS). Infrared spectra of KBr disks were recorded on a Nicolet Protégé-460 Fourier transform spectrophotometer. Elemental analyses of the nanocomposites were carried out with a Heraeus CHN-OS Rapid instrument. An X-ray diffraction study of the samples was carried out using a MAC Science MXP18 X-ray diffractometer (30 kV, 20 mA) with a copper target (λ = 1.54 Å) at a scanning rate of 4°/min. Thermal gravimetric analyses of the polyimide films were carried out with a Du Pont TGA 2950 at a heating rate of 20 °C/min with a nitrogen purge. Measurements of glass transition temperatures and coefficients of thermal expansion (CTE) for the films were carried out using a Du Pont TMA 2940 (film probe) at a heating rate of 20 °C/min in a nitrogen atmosphere. Samples for the transmission electron microscopy (TEM) study were first prepared by putting PMDA-ODA/POSS films into epoxy capsules and curing the epoxy at 70 °C for 48 h in a vacuum oven. Then, the cured epoxy samples were microtomed with a Leica Ultracut Uct into about 90 nm thick slices. Subsequently, a layer of carbon about 3 nm thick was deposited onto these slices and placed on mesh 200 copper nets for TEM observation. The TEM instrument used is a JEOL-2000 FX, with an acceleration voltage of 200 kV. The measured densities (d^M) of polyimide nanocomposite films were obtained by dividing the weight of the films by their volume. At least three specimens were used for each density data point. The relative porosity increase was calculated based on eq 1.

$$\text{Relative-porosity-increase } (\phi_r) = \underbrace{[(d^T - d^M)/d^T] \times 100\ \%}_{\text{due to packing}} + \underbrace{(0.048 \times V\ \%)}_{\text{due to porosity core of POSS}} \quad (1)$$

where d^T is the theoretical density of the POSS/polyimide nanocomposites estimated from the weight percentage of POSS in the nanocomposite and the density of POSS and polyimide (1.12 and 1.48 g/cm^3, respectively). V % is the volume percentage of POSS in the nanocomposites. The nanoporosity core of POSS with a diameter of 0.54 nm in a POSS molecule of 1.5 nm in diameter represents only 4.8 vol % of the total POSS volume as provided by the Hybrid Plastics Co. The dielectric constant measurements for PMDA-ODA and POSS/PMDA-ODA were carried out in a sandwich structure [aluminum (Al)/polyimide/platinum (Pt)] on a Si wafer. The top Al electrode, with an area of 1.0 × 0.8 mm^2, was deposited by thermal evaporation in a vacuum at 4 × 10^{-6} Pa on polyimide films, which were spun and imidized on a Si wafer plated with platinum. Then, these films were dried at 130 °C under vacuum for 2 days. The thicknesses of PMDA-ODA and POSS/PMDA-ODA films are about 3 μm. The capacitance of the samples was determined with a HP4280A at a frequency of 1 MHz. The dielectric constants of the samples can be calculated from their capacitances. The tensile properties of self-standing polyimide films were measured according to ASTM D882-88 at a crosshead speed of 2 mm/min.

Results and Discussion

Figure 1 shows ^{1}H NMR spectra of POSS-Cl, POSS-aldehyde, and POSS-diamine. For POSS-aldehyde, the three peaks at 7.1, 7.8, and 9.9 ppm result from the protons (d, e, and f) of the 4-hydroxybenzaldehyde moieties, confirming the formation of POSS-aldehyde. For POSS-diamine, two peaks at 6.6 and 6.8 ppm (h and g) appear, and peaks e and f are shifted upfield to 6.9 and 5.3 ppm, respectively. Additionally, matrix-assisted laser desorption ionization-time-of-flight mass spectrometry (MALDI−TOF MS) analysis results of POSS-aldehyde and POSS-diamine indicate dominant signals at m/z values of 1112.0 and 1279.1, respectively, which agree very well with the corresponding calculated values of 1110.3 and 1278.4.

Figure 2 presents NMR spectra of poly(amic acid) containing 16 mol % POSS. The two small peaks at 7.1 and 7.6 ppm are shifted downfield from 6.8 and 6.6 ppm, compared with the peaks (h and g) of POSS-diamine, which indicates that POSS-diamine has reacted with PMDA. FTIR spectra of polyimide containing 16 mol % POSS are given in Figure 3. The characteristic imide group bands at 1786 and 1725 cm^{-1} imply a fully imidized structure. The FTIR spectrum of 16 mol % POSS/polyimide shows Si−O−Si asymmetric stretching absorptions between 1000 and 1180 cm^{-1} and the aliphatic C−H stretching band between 2800 and 2900 cm^{-1}, confirming that POSS molecules are present in polyimide.

Table 1 presents the intrinsic viscosities and elemental analysis results of polyimide and POSS/polyimide nanocomposites. The intrinsic viscosities of poly(amic acid) in NMP at 30 °C are between 1.1 and 1.4 dL/g. The viscosities of POSS/PMDA-ODA nanocomposites are lower than that of pure PMDA-ODA but increase with the amount of POSS. The lower viscosities of the nanocomposites may be caused by the lower reactivity of POSS-diamine, as compared to that of ODA, and the increase in viscosity is due to the presence of POSS. The

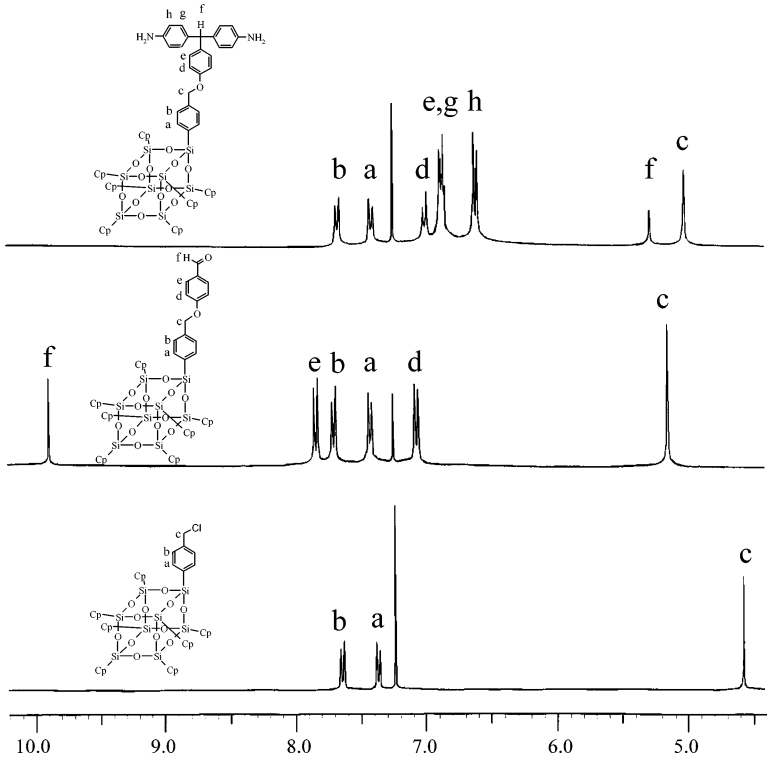

Figure 1. ^{1}H NMR spectra of (a) POSS-Cl, (b) POSS-aldehyde, and (c) POSS-diamine.

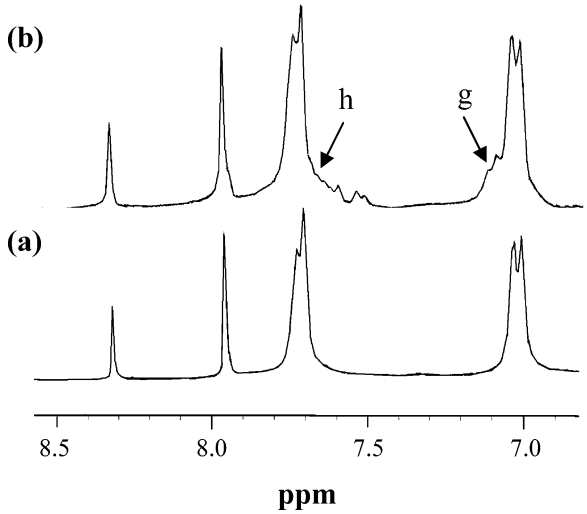

Figure 2. NMR spectra of poly(amic acid) of (a) PMDA-ODA and (b) 16 mol % POSS/PMDA-ODA.

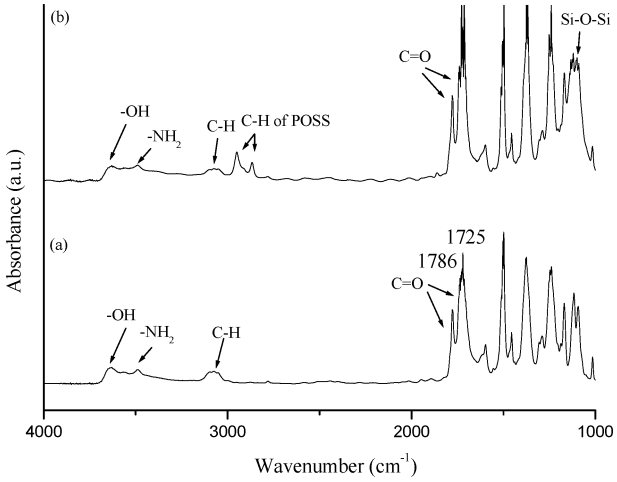

Figure 3. FTIR spectra of (a) PMDA-ODA and (b) 16 mol % POSS/PMDA-ODA.

actual amount of POSS molecules in polyimide is determined from the elemental analysis, and the volume percentage of POSS in polyimide is calculated from the densities of POSS and polyimide (1.12 and 1.48 g/cm^3, respectively).

Figure 4 shows the X-ray diffraction curves of POSS-diamine, polyimide, and POSS/polyimide nanocomposites. There are five distinct diffraction peaks at 2θ = 8.3°, 11.3°, 19.1°, and 25.9° by POSS-diamine, corresponding to *d*-spacings of 10.5, 7.2, 4.6, and 3.3 Å, respectively. The peak corresponding to a *d*-spacing of 10.5 Å is caused by the size of POSS-diamine molecules; the remaining peaks are produced by the rhombohedral crystal structure of POSS molecules.[21] No X-ray diffraction peak is obtained for pure polyimide. A small but broad peak at 2θ = 8° is also observed in the diffraction curves of POSS/polyimide, indicating that one dimension of the POSS molecules remains approximately 1 nm in polyimide.

Figure 5a−c shows the morphologies of cross sections of POSS/polyimide nanocomposites obtained by transmission electron microscopy. In Figure 5a, the 5 mol % case, darker points represent POSS molecules, and the distribution of these points is roughly concentrated in a small region in the right bottom corner of the micrograph. For the 10 mol % POSS case, random domains of parallel dark lines consisting of POSS molecules about 2 nm thick are formed, as shown in Figure 5b. This phenomenon is a result of self-assembled POSS molecules. The POSS self-assembly is most likely caused by the chain-to-chain arrangement of POSS molecules and polyimide chains, since polar−polar interactions between imide segments (O═C−N) are quite different from van der Waals interactions between the cyclopentyl groups of POSS molecules. For

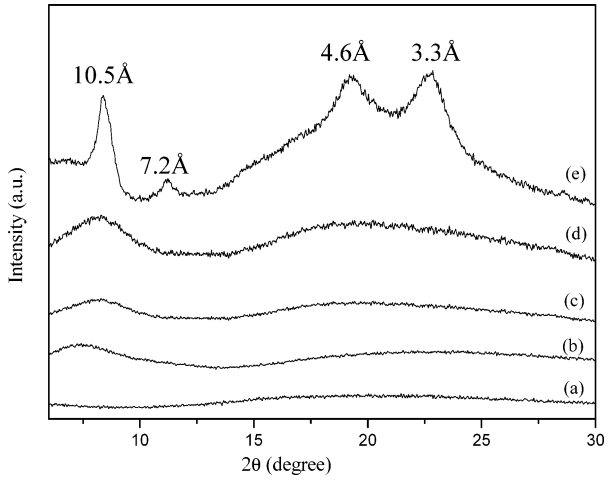

Figure 4. X-ray diffraction curves of (a) PMDA-ODA, (b) 5 mol % POSS/PMDA-ODA, (c) 10 mol % POSS/PMDA-ODA, (d) 16 mol % POSS/PMDA-ODA, and (e) POSS-diamine.

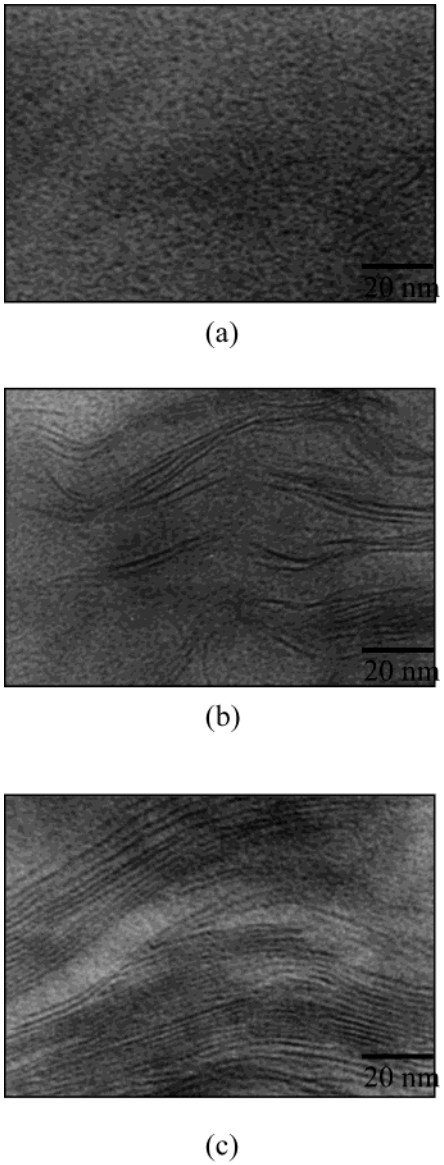

Figure 5. Transmission electron micrographs of cross sections of (a) 5 mol %, (b) 10 mol %, and (c) 16 mol % POSS/PMDA-ODA nanocomposites.

the 16 mol % POSS case, a large scale self-assembled layer-by-layer structure of POSS was revealed, as illustrated in Figure 5c. This structure possesses a layer length greater than 100 nm and layer spacings of about 2−4 nm. A schematic drawing of the architecture of polyimide-tethered POSS is given in Figure 6. The sizes of POSS and polyimide molecules are approximately 1 and 50 nm, respectively.

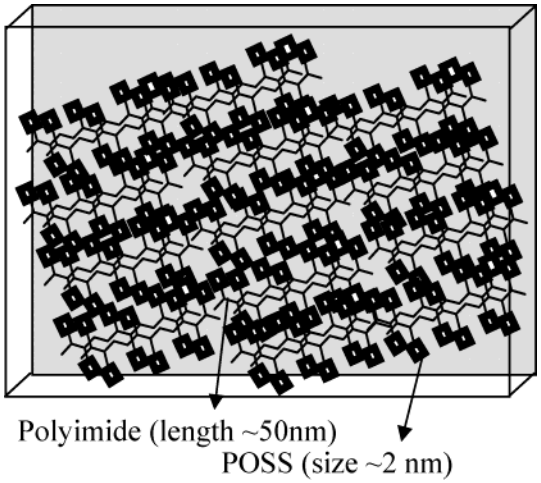

Figure 6. Schematic drawing of the self-assembled architecture of polyimide-tethered POSS.

Table 2. Densities and Dielectric Constants of POSS/Polyimide Nanocomposites

mol % of POSS in polyimide	dielectric constant	theor density (d^T) (g/cm^3)	measd density (d^M) (g/cm^3)	rel porosity increase (ϕ_r) (%)
0	3.26 ± 0.09	1.48	1.48 ± 0.02	0
5	2.86 ± 0.04	1.41	1.39 ± 0.02	2.3
10	2.57 ± 0.08	1.35	1.32 ± 0.01	3.8
16	2.32 ± 0.05	1.30	1.24 ± 0.03	6.8

Table 2 presents the dielectric constants and densities of the POSS/polyimide nanocomposites. The dielectric constants of the POSS/polyimide nanocomposites decrease as the amount of POSS increases. The maximum reduction in the dielectric constant of POSS/polyimide nanocomposites is about 29%, by comparing 16 mol % POSS/polyimide to pure polyimide (k = 2.32 vs 3.26). There are a few possible causes for the reduction in the dielectric constant. Since the porosities of these nanocomposite films are difficult to obtain (the size distribution of pores cannot be detected by small-angle X-ray scattering), we adopt a simple method to measure the relative porosities of these films. The relative porosity increase (ϕ_r) is defined as the sun of increased external porosity due to the incorporation of POSS molecules in polyimide and the nanoporosity of POSS molecules themselves and is calculated based upon eq 1 given earlier. ϕ_r for the 16 mol % POSS/polyimide case is 6.8%; this ϕ_r value, however, cannot possibly account for the entire 29% reduction in the dielectric constant of the nanocomposite film. Hence, the reduction is most likely due to the nanoporosity in the core of POSS molecules[7] and the external porosity introduced by tethering POSS to the polyimide, as evidenced by the decreasing density and the increasing value of ϕ_r for the nanocomposite films when the amount of POSS in the film increases. The increase in the external porosity in the nanocomposites as a result of POSS molecules in turn can be further interpreted as an increase in the free volume of the nanocomposites because of the interaction of polyimide segments and tethered POSS.[25] The increase in the free volume of polyimide corresponds to the fact that

Table 3. Thermal and Mechanical Properties of Self-Standing POSS/Polyimide Films

mol % of POSS in polyimide	T_d (°C) at 5 wt % loss[a]	T_g[b] (°C)	CTE (ppm) 50−200 °C	Young's modulus (GPa)	break elongation (%)	max stress (MPa)
0	604.6	350.7	31.9	1.60 ± 0.07	6 ± 1	50.9 ± 1.2
5	583.7	316.6	49.7	1.58 ± 0.08	5 ± 1	48.9 ± 5.1
10	552.4	308.1	54.4	1.43 ± 0.07	4 ± 1	46.4 ± 7.9
16	534.5	303.9	57.1	1.25 ± 0.04	2 ± 1	20.4 ± 1.1

[a] T_d: thermal degradation temperature at 5 wt % loss. [b] T_g: glass transition temperature.

the glass transition temperature (T_g) of the polyimide in the nanocomposites is lower than that of the pure polyimide quite well. A second cause is that the POSS molecules are simply less polar than imide segments, which in turn reduces the dielectric constant of the nanocomposites.

The degradation temperatures (T_d) of POSS/polyimide nanocomposites, shown in Table 3, are lower than that of pure polyimide due to the degradation of cyclopentyl groups on POSS molecules (at ∼400 °C). The in-plane coefficient of thermal expansion of POSS/polyimide nanocomposites increases with the amount of POSS as a result of the increase in the free volume in polyimide due to POSS molecules.

Table 3 also shows a slight reduction (about 4%) in the tensile properties for the 5 mol % POSS/polyimide case as compared to that of pure polyimide, owing to the rigidity of POSS. As the amount of POSS increases to 10 mol %, the decrease in Young's modulus, maximum stress, and maximum elongation become more apparent (about 10%), but the dielectric constant of the nanocomposite reduces by more than 20% (2.57vs 3.26). Hence, the overall properties of polyimide-tethered POSS nanocomposites indicated that it is possible to have a substantially lower dielectric constant at the expense of substantially decreased mechanical properties for these nanocomposites, as compared to the pure polyimide case.

Conclusion

Polyimide-tethered POSS nanocomposites with well-defined architectures are prepared by the reaction of a new type of diamine monomer, POSS-diamine, and other diamines with dianhydride monomers. POSS molecules tethered to polyimide form self-assembled architecture as the mole ratio of POSS is more than 10%. The dielectric constant of the resulting nanocomposites are lower and can be tuned by varying the molar ratio of POSS; polyimide molecules offer additional advantages of maintaining certain thermal and mechanical strengths.

Acknowledgment. We appreciate the financial support provided by the National Science Council through Project NSC 91-2120-M-009-001.

References and Notes

(1) Feger, C.; Franke, H. In *Polyimides Fundamentals and Applications*; Ghosh, M. K., Mittal, K. L., Eds.; Marcel Decker: New York, 1996; pp 759−814.
(2) Haider, M.; Chenevey, E.; Vora, R. H.; Cooper, W.; Glick, M.; Jaffe, M. *Mater. Res. Soc. Symp. Proc.* **1991**, *227*, 379.
(3) Auman, B. C.; Trofimenko, S. *Polym. Prepr. (Am. Chem. Soc., Div. Polym. Chem.)* **1992**, *34* (2), 244.
(4) Auman, B. C. In *Advances in Polyimide Science and Technology*; Proceedings of the 4th International Conference on Polyimides, 1991.
(5) Carter, K. R.; DiPietro, R. A.; Sanchez, M. I.; Russell, T. P.; Lakshmanan, P.; McGrath, J. E. *Chem. Mater.* **1997**, *9*, 105.
(6) Carter, K. R.; DiPietro, R. A.; Sanchez, M. I.; Swanson, S. A. *Chem. Mater.* **2001**, *13*, 213.
(7) Zhang, C.; Babonneau, F.; Bonhomme, C.; Laine, R. M.; Soles, C. L.; Hristov, H. A.; Yee, A. F. *J. Am. Chem. Soc.* **1998**, *120*, 8380.
(8) Lichtenhan, J. D.; Vu, N. Q.; Carter, J. A.; Gilman, J. W.; Feher, F. J. *Macromolecules* **1993**, *26*, 2141.
(9) Lichtenhan, J. D.; Otonari, Y. A.; Carr, M. J. *Macromlecules* **1995**, *28*, 8435.
(10) Haddad, T. S.; Lichtenhan, J. D. *Macromolecules* **1996**, *29*, 7302.
(11) Lee, A.; Lichtenhan, J. D. *Macromolecules* **1970**, *3*, 4970.
(12) Feher, F. J.; Soulivong, D.; Eklud, A. G.; Wyndham, K. D. *Chem. Commun.* **1997**, 1185.
(13) Fu, B. X.; Zhang, W. H.; Hsiao, B. S.; Rafailovich, M.; Sokolov, J.; Sauer, B. B.; Phillips, S.; Balnski, R. *High Perform. Polym.* **2000**, *12*, 565.
(14) Jeon, H. G.; Mather, P. T.; Haddad, T. S. *Polym. Int.* **2000**, *49*, 453.
(15) Haddad, T. S.; Mather, P. T.; Jeon, H. G.; Romo-Uribe, A.; Farris, R.; Lichtenhan, J. D. In *Organic/Inorganic Hybrid Materials*; Laine, R., Sanchez, Brinker, Giannelis, Eds.; MRS Symp. Ser. 519; Materials Research Society: Warrendale, PA, 1998; pp 381−386.
(16) Gilman, J. W.; Schlitzere, D. S.; Lichtenhan, J. D. *J. Appl. Polym. Sci.* **1996**, *60*, 591.
(17) Gonzalez, R. I.; Phillips, S. H.; Hoflund, G. B. *J. Spacecr. Rockets* **2000**B, *37*, 463.
(18) Laine, R. M.; Choi, J.; Lee, I. *Adv. Mater.* **2001**, *13*, 800.
(19) Zhang, C.; Laine, R. M. *J. Am. Chem. Soc.* **2000** *122*, 6979.
(20) Tamaki, R.; Tanaka, Y.; Asuncion, M. Z.; Choi, J.; Laine, R. M. *J. Am. Chem. Soc.* **2001**, *123*, 12416.
(21) Zheng, L.; Waddon, A. J.; Farris, R. J.; Coughlin, E. B. *Macromolecules* **2002**, *35*, 2375.
(22) Choi, J.; Tamaki, R.; Kim, S. G.; Laine, R. M.*Chem. Mater.* **2003**, *15*, 793.
(23) Leu, C. M.; Reddy, G. M.; Wei, K. H.; Shu, C. F. *Chem. Mater.* **2003**, *15*, 2261.
(24) Leu, C. M.; Chang, Y. T.; Wei, K. H. *Chem. Mater.* **2003**, *15*, 3721.
(25) Merkel, T. C.; Freeman, B. D.; Spontak, R. J.; He, Z.; Pinnau, I.; Meakin, P.; Hill, A. *Science* **2002**, *296*, 519.

MA034743R